

# Persistent currents and quantised vortices in a polariton superfluid

D. Sanvitto,<sup>1,\*</sup> F. M. Marchetti,<sup>2,†</sup> M. H. Szymańska,<sup>3,‡</sup> G. Tosi,<sup>1</sup>  
M. Baudisch,<sup>1</sup> F. P. Laussy,<sup>4</sup> D. N. Krizhanovskii,<sup>5</sup> M. S. Skolnick,<sup>5</sup>  
L. Marrucci,<sup>6</sup> A. Lemaître,<sup>7</sup> J. Bloch,<sup>7</sup> C. Tejedor,<sup>2</sup> and L. Viña<sup>1</sup>

<sup>1</sup>*Departamento de Física de Materiales,*

*Universidad Autónoma de Madrid, Madrid 28049, Spain*

<sup>2</sup>*Departamento de Física Teórica de la Materia Condensada,*

*Universidad Autónoma de Madrid, Madrid 28049, Spain*

<sup>3</sup>*Department of Physics, University of Warwick, Coventry, CV4 7AL, UK*

<sup>4</sup>*Physics and Astronomy, University of Southampton, Southampton, SO17 1BJ, UK*

<sup>5</sup>*Department of Physics and Astronomy,*

*University of Sheffield, Sheffield, S3 7RH, UK*

<sup>6</sup>*Dipartimento di Scienze Fisiche, Università di Napoli*

*Federico II and CNR-INFN Coherentia, Napoli, Italy*

<sup>7</sup>*LPN/CNRS, Route de Nozay, 91460, Marcoussis, France*

(Dated: April 11, 2019)

Semiconductor microcavity polaritons in the optical parametric scattering regime have been recently demonstrated to display a new variety of dissipationless superfluid behaviour. We report the first observation in resonantly pumped exciton polaritons of a metastable persistent superflow carrying quantum of angular momentum,  $m$ . The quantised vortex, excited by a weak 2ps pulsed probe, is shown to last for at least 80ps, limited only by the leaking outside the cavity. The polariton circulating superfluid persists in the absence of the driving rotating probe with no apparent dissipation. In addition, for a moving superfluid, we show the coherent splitting of a quantised double vortex, with charge  $m = 2$ , into two singly quantised vortices of  $m = 1$ . Remarkably, we observe the  $m = 2$  vortex to be stable when they are at rest. The experimental results are compared with a theoretical analysis, obtained describing the triggered parametric scattering regime of polaritons via a two-component Gross-Pitaevskii equation, including pump and decay processes.

In the past few decades there has been a strenuous search for macroscopic coherence and phenomena related to Bose-Einstein condensation (BEC) in the solid state. The first realisation of a BEC in semiconductor microcavities [1] has inaugurated a new era in the study of strongly coupled light-matter systems. The growing interest in this field can be attributed to the unique properties of exciton polaritons in microcavities [2], the composite particles resulting from strong light-matter interactions. Properties of a polariton condensate [3] differ from that of other known condensates, such as ultracold atomic BECs and superfluid  $^4\text{He}$ . In particular, polaritons have a short life time of the order of picoseconds, therefore needing continuous pumping to balance decay and reach a steady state regime. Rather than a drawback, the intrinsic non-equilibrium nature enriches the features of polariton condensation, but at the same time poses fundamental questions about the robustness of the coherence phenomena to dissipation and non-equilibrium. Superfluid properties of non-equilibrium condensates in dissipative environment still need to be understood [4] and this letter provides a substantial advance in this direction.

One route to experimentally inject polaritons into a microcavity is by non-resonant (incoherent) pumping. For incoherent pumping, polaritons have been shown to enter, within their short lifetime, a macroscopically coherent BEC phase [1, 5]. As a consequence of non-equilibrium currents in an inhomogeneous system, carrying particles from gain to loss

dominated regions, deterministic quantised vortices have been observed to spontaneously appear [6]. However, the unusual—diffusive at small momenta—form of the excitation spectrum [7, 8], which hinders the fulfilling of the Landau criterion, puts under debate the possibility of dissipationless superflow in incoherently pumped polariton systems.

A different scenario characterises coherent resonant injection of parametrically pumped polariton condensates, which have been recently shown to exhibit a new form of non-equilibrium superfluid behaviour [9, 10]. In the optical parametric oscillator (OPO) regime [11], bosonic final state stimulation causes polariton pairs to coherently scatter from the pump state to the signal and idler states, which, at threshold, have a state occupancy of order one. The properties of the quantum fluids generated by OPO at idler and signal have been recently tested via a triggered optical parametric oscillator (TOPO) configuration [9]. An additional weak pulsed probe laser beam has been used to create a traveling, long-living, coherent polaritons signal, continuously fed by the OPO. The traveling signal has been shown to display superfluid behaviour through linear dispersion and frictionless flow. However, generating long-lived quantised vortices and the possibility of metastable persistent flow in this configuration still remain missing in the superfluid ‘checklist’ [4].

We show for the first time that the non-equilibrium superfluid generated with a TOPO can hold a vortex state carrying angular momentum with quantum number  $m$ , and this is observed up to 80ps after the probe has been switched off, more than 10 times the lifetime of photons in the microcavity. The vortex is excited by a weak, pulsed probe resonant with the signal (see Fig. 1) lasting 2ps only. In other words we stir the polariton superfluid only for a short time and observe its long lived rotation with the identical quantum of angular momentum on a time scale almost 40 times longer than the duration of the pulse (see Figs. 2 and 3), the analogous of the *rotating drive* in trapped gases. Thus in this work, we observe two of the most fundamental properties of a superfluid: Quantisation of circulation and stability of persistent currents in the novel non-equilibrium and dissipative system of driven polariton condensates, demonstrating robustness of superfluid phenomena.

Another fundamental property of vortices with higher charge number  $m$  observed in atomic superfluids, is the tendency to coherently split into many vortices of charge  $m = 1$ . To study the stability properties of vortices in polariton condensates, we have injected a vortex with  $m = 2$  and let it evolve within the time of observation (see Fig. 4). Surprisingly, we found that the vortex splits only when it is moving. Indeed, dynamic instability of doubly

quantised vortices, in atomic BEC, has been observed [12], where a double quantised vortex has been showed to coherently break into two singly quantised vortices. However, there are few systems where double quantised vortices have been shown to be stable, for example in superconductors in the presence of pinning forces [13], and in superfluid  $^3\text{He-A}$ , which has a multicomponent order parameter [14]. Remarkable stability of  $m = 2$  static vortex in polariton systems provides an additional example.

In our experiment we use a semiconductor microcavity with a Rabi splitting  $\Omega_R = 4.4\text{meV}$  and the cavity photon energy slightly negatively detuned below the exciton energy,  $\delta \in [-3, -1]\text{meV}$ —for details see the Method section—. A Ti-Sapphire laser is tuned in resonance with the lower polariton branch (LPB), injecting polaritons close to the point of inflection and giving rise to a continuously pumped OPO (see Fig. 1). Above a pump threshold, the generated signal state close to zero momentum ( $\mathbf{k}_s = 0$ ) as well as the idler state at high momentum, form an out of equilibrium coherent polariton superfluid. At a given time we trigger a new scattering process on top of the OPO (TOPO) signal with a resonant pulsed probe smaller than the signal. The probe is a pulsed Laguerre-Gauss beam carrying a vortex of given angular momentum  $m$ , the phase of which winds around the vortex core with values from 0 to  $2\pi m$ . However, after a short time,  $\sim 2\text{ps}$ , we remove the probe, leaving the polariton coherent state free to rotate, without the driving field. While even a classical fluid acquires angular momentum in the presence of an external rotating drive, only a superfluid can exhibit long lived circulating flow once the external drive is turned off.

In order to demonstrate persistence of the vortex angular momentum, we detect the phase pattern generated by making interfere the TOPO signal with an expanded and flipped spatial region far from the vortex core (where the phase is approximately constant) in a Michelson interferometer. A fork-like dislocation with a difference of  $m$  arms corresponds to phase winding by  $2\pi m$  around the vortex core (see lower panel of Fig. 1).

Using a streak camera we can follow the evolution in time of the vortex generated by the pulsed probe. Time intervals of 1 or 2ps are used to reconstruct 2D images of the signal state after the perturbation has arrived. Every picture is the result of an average over many shots, all taken at the same time and same conditions. In order to separate the contribution of the signal from that of the pump, both in theory and experiments, we filter the signal images in momentum space in a cone around  $\mathbf{k} = 0$  of approximately  $\pm 7^\circ$ .

The time evolution of an excited  $m = 1$  vortex together with its interference pattern,

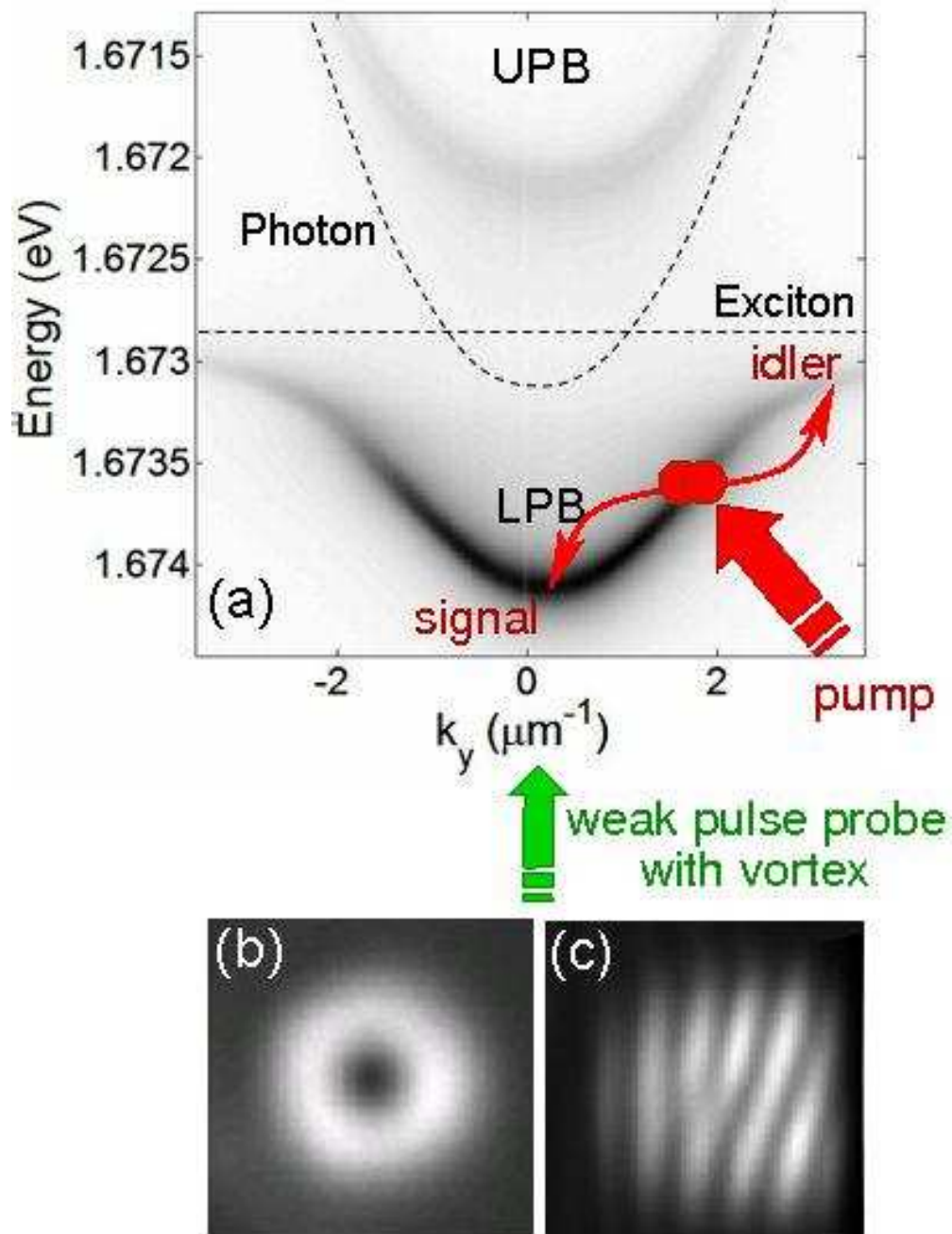


FIG. 1: Lower (LPB) and upper polariton branch (UPB) dispersions together with the schematic representation of the TOPO excitation (a). Resonantly pumping the LPB initiates, above threshold, stimulated scattering to a signal close to zero momentum and an idler at higher momentum. The  $m = 1$  Laguerre-Gauss beam resonant with the signal (b) is used as a weak pulsed triggering probe to stir the superfluid. The corresponding interference image is shown in panel (c).

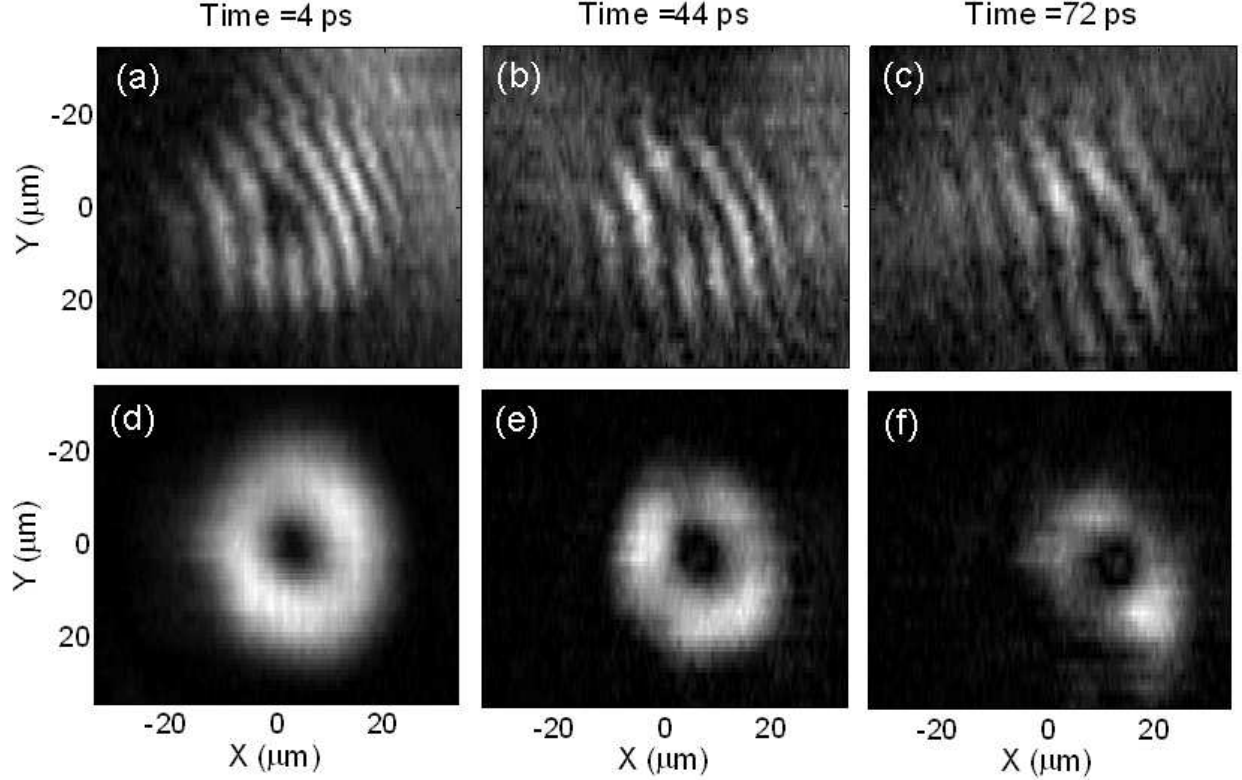


FIG. 2: Time evolution of the TOPO signal after a weak pulsed probe with a vortex of  $m = 1$  has been excited (d-f). The corresponding interference images (a-c) are obtained by overlapping the vortex with a small expanded region of the same image far from the vortex core, where the phase is constant. The time origin is taken when the TOPO has reached 80% of its maximum value.

which characterises unequivocally the vortex state, are shown in Figure 2. The probe has a power of 0.3mW which is comparable to the OPO signal emission intensity, before the probe arrives on the sample at time  $t_{pb}$ . The effect of the probe is to enhance the polariton signal emission by a factor of 20 with a delay of 10ps after the pulse arrival time. The vortex appears as a new state on top of the OPO signal. To eliminate the contribution of the steady state, we subtract the emission of the OPO in absence of the probe pulse. The signal generated by this perturbation lasts about a hundred picoseconds.

The images of Fig. 2 demonstrate that the effect of the probe on the signal steady state is lasting for at least 80 picoseconds after the probe is switched off, and during this time we observe a circular flow of polaritons rotating unperturbed. This effect is visible in the real space images through the ‘thoroidal shape’ of the polariton emission which is present

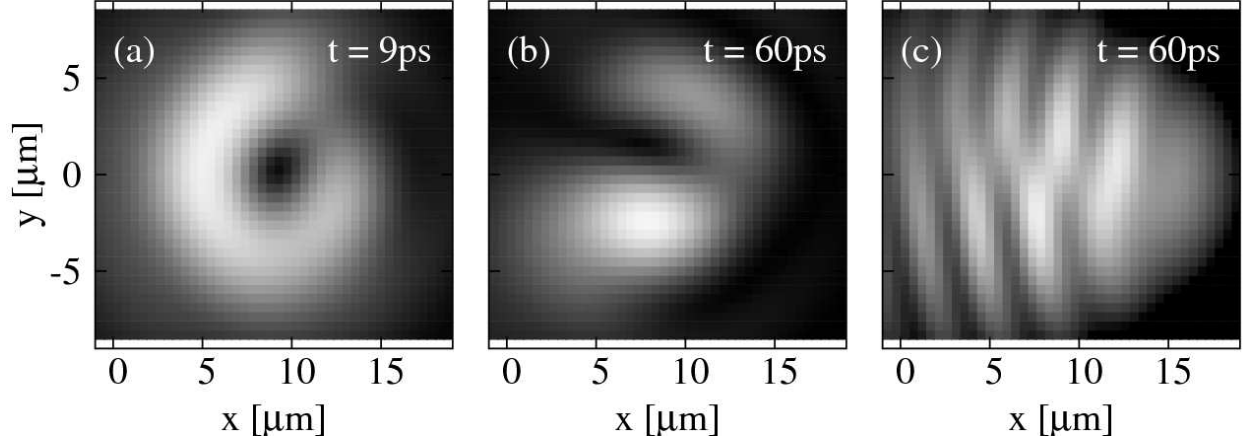


FIG. 3: Numerical simulations of the time evolution of the TOPO signal after a weak pulsed probe with a vortex of  $m = 1$  has been impinged at  $\mathbf{k} = 0$ , and for pumping strength very close to the OPO threshold ( $f_p = 0.999 f_p^{(\text{th})}$ ). (a) and (b) show images of the signal obtained by momentum filtering in a cone of around  $7^\circ$ , while interference fringes of (c), showing the characteristic fork-like dislocation of the  $m = 1$  vortex, are obtained by taking the full emission without filtering out the pump.

at any time. During the time the vortex lasts, we can observe the vortex slowly drifting to the right and changing slightly its shape. The drift is due to the fact that the probe has a small component at finite positive momentum. The small changes in time of the polariton vortex shape are due to the presence of local defects [15], which tends to influence the polariton density distribution around the vortex core, affecting therefore the shape of the excited vortex. However, the interference pattern clearly shows that the spatial phase relation, including the fork dislocation, remains constant and with full contrast all over a wide area, even for times when the interference contrast of the signal polariton has dropped down to 30% due to the relatively short (50ps) polariton coherence time—see figure in the supplementary material—. This means that even when polaritons have lost any phase relation in time, the angular momentum is still conserved.

The sequence in Figure 2 demonstrates that the vortex remains steady as a persisting metastable state as long as the extra population, created by the probe, lasts. Eventually the system will tend to the steady state and all angular momentum will be transferred to the photons leaking out of the cavity. However, down to the last detectable signal we

observe a decrease of vortex radius and intensity but no loss of winding number due to dissipation. This is revealed by the strong contrast of the fork in the interference images. In the opposite scenario, the interference images would show low contrast in the vortex core region, indicating a mixture of the population which has undergone dissipation and the one still carrying the quantised angular momentum.

We have numerically simulated the experiments by making use of mean-field two-component Gross-Pitaevskii equations for the coupled cavity and exciton fields with external pump and decay—see also Method section—. In order to reproduce conditions similar to the experimental ones (TOPO), where the vortex appears as a new state on top of the OPO signal, we choose parameters very close to the OPO threshold from below. Under these conditions we observe the weak pulsed probe to trigger a vortex state at the signal which can last around 80ps (see Fig. 3), in agreement with the experimental results. Images of the vortex are obtained by filtering in momentum space. Interference fringes showing the characteristic fork-like dislocation of the  $m = 1$  vortex are obtained by taking the full emission without filtering out the pump. Like in the experiments, we observe the vortex state lasting as long as the signal lasts. In contrast, a vortex created at  $\mathbf{k} = 0$  well below the OPO threshold, typically decays already two orders of magnitude in intensity within the firsts 20ps.

A second experiment aimed at investigating the stability of doubly charged vortices in different regimes. Therefore, we repeat both our experiments and simulations in conditions similar to the ones previously described, but now generating a TOPO doubly quantised vortex, i.e. with  $m = 2$ . By repeating the experiment in a variety of different conditions, we observe that when the vortex is excited on a static signal centered at  $\mathbf{k} = 0$  the vortex does not split within its lifetime. However, exciting the TOPO signal with a finite momentum, thus making it moving inside the pump spot, we observe the doubly quantised vortex splitting into two singly quantised vortices as shown in Fig. 4. Our theoretical analysis gives the same result: vortex at rest is stable while a moving vortex splits (see lower panels in Fig. 4), obtained under the same conditions as in Fig. 3. Splitting occurs when the vortex starts slowly drifting in space and the signal emission becomes asymmetric around  $\mathbf{k} = 0$ , which happens around 6ps after the probe has been switched off. The splitting of the vortex is confirmed by the interference image.

In the numerical simulations, we also observed a qualitatively different regime in which

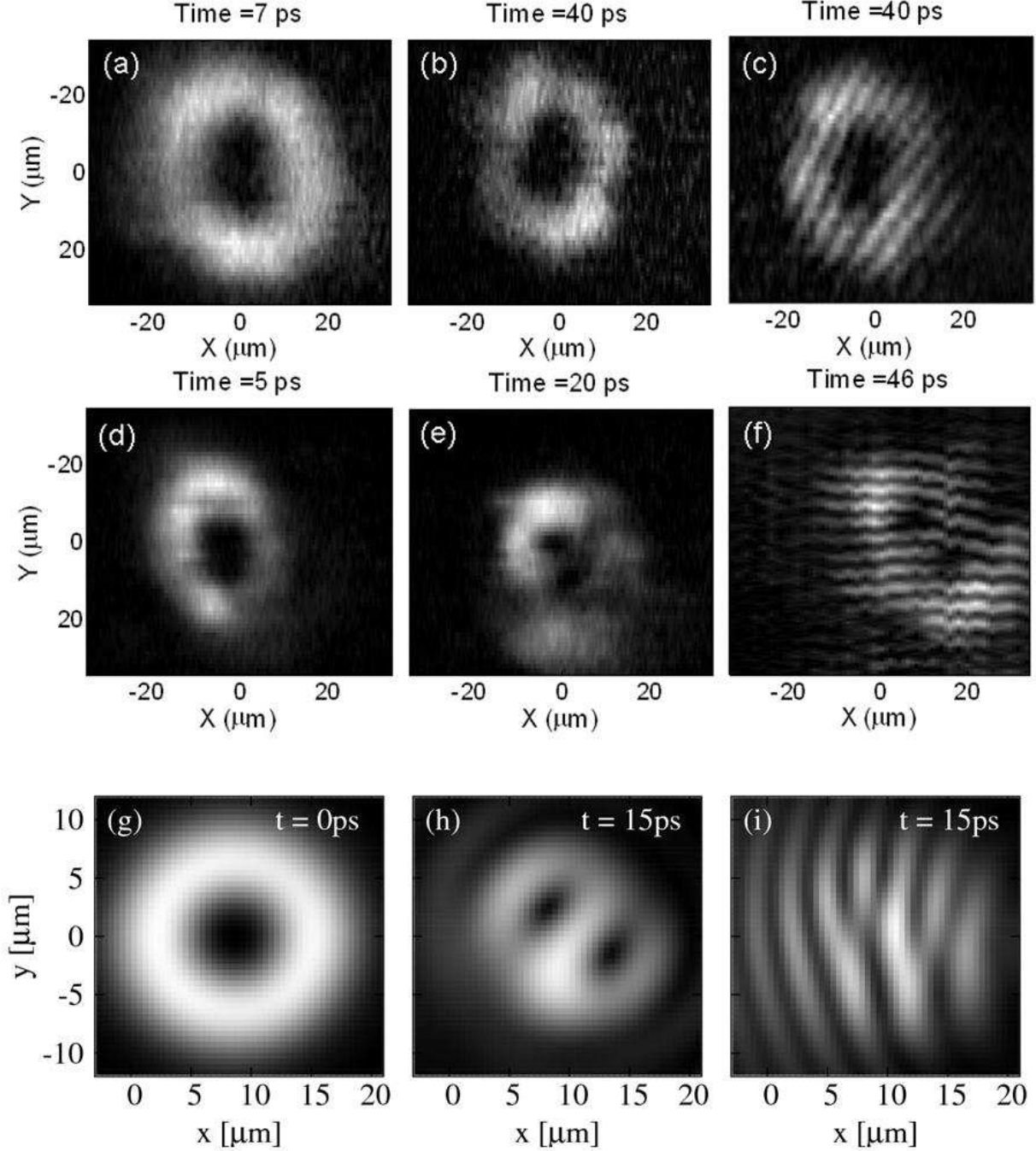


FIG. 4: Time evolution of a  $m = 2$  vortex TOPO signal excited close to zero momentum,  $|\mathbf{k}| = 0$ , (a-c) for which neither motion nor splitting of the vortex could be detected. However for a signal at  $\mathbf{k}_s$  pointing to the right (d-f), we can detect the  $m = 2$  vortex both moving and splitting into two single quantised  $m = 1$  vortices. Numerical simulations of the time evolution of the TOPO signal in the same conditions of Fig. 3 (g-i). The doubly quantised vortex splits already after 6ps the probe has been switched off, corresponding to the moment at which the vortex starts also drifting. In the last panel of each row we plot the interference

very long lived vortices are found to appear in the steady state signal, following the probe pulse. In the simulation of Fig. 5, once the OPO steady state is reached, we turn on the probe resonant with the OPO signal for 2ps only. After the probe is switched off, the signal experiences a transient period, when either the vortex drifts around or no vortex can be detected. After the transient, independently on the intensity and size of the probe, a vortex with a quantum of angular momentum stabilises into the signal and lasts as long as our simulations ( $\sim 1$ ns). We have observed stable vortex solutions for probe intensities down to 1/20 the intensity of the signal and also for different vortex probe sizes. A stable vortex solution does not always exist; there are cases where, during the transient period, the excited vortex spirals out of the signal. Stable vortex solutions above the OPO threshold were also reported in Ref. [16].

By contrast, in experiments, vortices in the steady state regime are not detected. One possibility could be that disorder can pin the phase of the signal OPO, thus making it harder for the probe to change the signal phase. A second reason could be that the presence of random noise (temperature and laser power fluctuations, normal fluid component, etc.) can contribute to give different dynamical scenarios at any experimental shot, depending on the initial conditions. Indeed, differently from the simulations, the experimental images are obtained by accumulating over several million realizations of the experiment, hiding the different final spatial configuration of the stable vortex in the signal OPO. However, in case of the TOPO configuration, the experiments start always with the same initial condition, which is imposed by the probe and kept by the driving field, and there is no transient period. Moreover, the presence of a strong OPO signal, which fills the sample inhomogeneities, strongly contributes in smoothing local defects, helping the free rotation of the triggered polariton condensate.

To conclude, we have demonstrated the presence of long lived quantised currents in a polariton superfluid which last as long as polaritons are present in that state. Our report is the first observation of persistent currents in semiconductors. The superfluid phenomena observed in our microcavity is shown to be robust despite the relatively large sample temperature (10K) and the presence of strong decay and dissipation. Moreover, the unexpected stability of winding number  $m = 2$  static vortices observed in this work, as well as our theoretical prediction of having, above OPO threshold, an imprinting into the OPO signal of the winding number of the probe, indicate the richness of superfluid behaviours which

can be realised with driven polariton condensates.

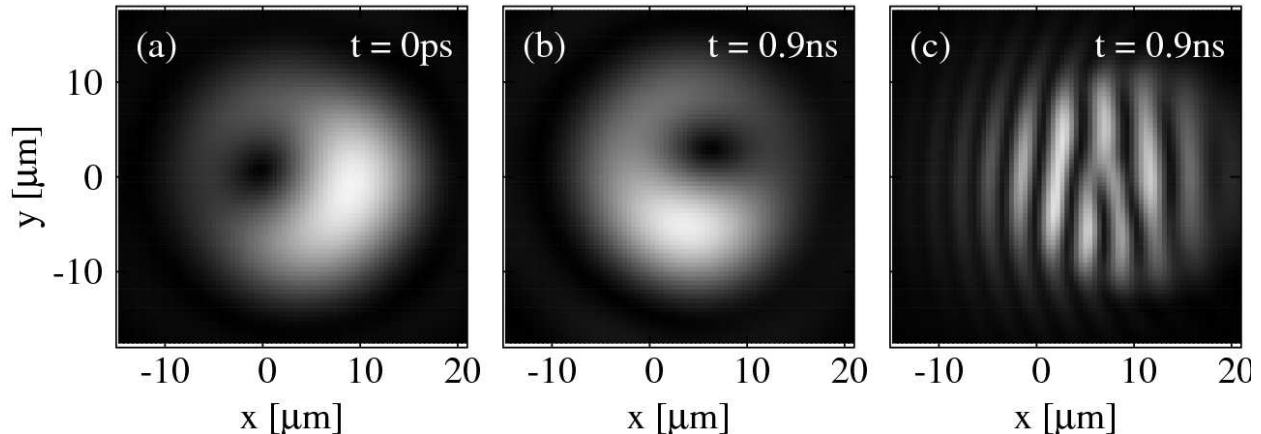


FIG. 5: Simulations showing the persistent vortex supercurrent with one quantum of angular momentum,  $m = 1$ , imposed with a short, pulsed vortex probe at the OPO signal, for pump strength above threshold  $f_p = 1.12f_p^{(\text{th})}$ . Simulations show the existence of a stable vortex solution even  $\sim 1$ ns after the driving probe has been removed.

## METHODS SUMMARY

In our TOPO experiment [9], the pump power was kept always above threshold for the OPO, in a pumping regime where the energy renormalisation around the spot area due to interaction is as constant as possible. The vortex probe state is prepared by scattering a pulsed laser Gaussian beam in an hologram with a single or double fork-like dislocation. This gives rise to a first order Laguerre-Gauss beam with a winding number respectively either  $m = 1$  or  $m = 2$ . The probe beam is focused at the center of the cw pump in resonance with the signal emission energy and at around  $\mathbf{k} = 0$ . Every picture is the result of an average over many shots, as single shot measurements would give a too low signal to noise ratio.

The dynamics of amplitudes and phases of TOPO is computed with a two-component Gross-Pitaevskii equation with external pumping and decay for the coupled cavity and exciton fields  $\psi_{C,X}(\mathbf{r}, t)$  ( $\hbar = 1$ ):

$$i\partial_t \begin{pmatrix} \psi_X \\ \psi_C \end{pmatrix} = \begin{pmatrix} \omega_X - i\kappa_X + g_X|\psi_X|^2 & \Omega_R/2 \\ \Omega_R/2 & \omega_C - i\kappa_C \end{pmatrix} \begin{pmatrix} \psi_X \\ \psi_C \end{pmatrix} + \begin{pmatrix} 0 \\ F_p + F_{pb} \end{pmatrix}. \quad (1)$$

Since the exciton mass is four orders of magnitude larger than the photon mass, we neglect the excitonic dispersion and assume a quadratic dispersion for the cavity photon,  $\omega_C = \omega_C(0) - \frac{\nabla^2}{2m_C}$ . The fields decay with rates  $\kappa_{C,X}$ .  $\Omega_R$  is the photon-exciton coupling. The cavity field is driven by an external cw pump field,

$$F_p(\mathbf{r}, t) = f_p e^{-\frac{|\mathbf{r}-\mathbf{r}_p|^2}{2\sigma_p^2}} e^{i(\mathbf{k}_p \cdot \mathbf{r} - \omega_p t)},$$

while the probe is a Laguerre-Gaussian pulsed beam,

$$F_{pb}(\mathbf{r}, t) \simeq f_{pb} |\mathbf{r} - \mathbf{r}_{pb}|^m e^{-\frac{|\mathbf{r}-\mathbf{r}_{pb}|^2}{2\sigma_{pb}^2}} e^{im\varphi(\mathbf{r})} e^{-\frac{(t-t_{pb})^2}{2\sigma_{pb}^2}} e^{i(\mathbf{k}_{pb} \cdot \mathbf{r} - \omega_{pb} t)}, \quad (2)$$

producing a vortex at  $\mathbf{r}_{pb}$  with winding number  $m$ . The exciton repulsive interaction strength  $g_X$  can be set to one by rescaling fields and pump strengths. We solve Eq. (1) numerically by using the 5<sup>th</sup>-order adaptive-step Runge-Kutta algorithm on a 2D grid.

## METHODS

### Experiments

The sample studied is a  $\lambda/2$  AlAs microcavity with a 20 nm GaAs quantum well placed at the antinode of the cavity electromagnetic field. The cavity is formed by two high reflective Bragg mirrors of 25 pairs at the bottom and 15.5 on the top of the structure. The pump is obtained with a cw Ti-Sapphire laser, resonantly exciting the LPB close to the inflection point at  $9^\circ$ . The spot size is of  $\approx 150\mu\text{m}$ . A pulsed Ti-Sapphire laser excites a probe 2ps long focussed to a diameter  $\approx 250\mu\text{m}$ .

The experiments are performed at a cryogenic temperature of 10 K and using a very high numerical aperture lens (0.6) so that the sample could be accessed by angles as large as  $25^\circ$  and the photoluminescence (PL) can be simultaneously collected from the signal state in the near as well as the far field. The PL was collected through a 0.5m spectrometer into a streak camera, working in synchroscan mode, with 4ps time resolution, allowing for energy- as well as time-resolved images. In order to reach high time resolution, all the images were obtained by filtering the signal in the far field without spectrally resolving the emission of the OPO states.

## Theory

In our numerical simulations, we take  $m_C = 2.3 \times 10^{-5} m_0$  and a Rabi splitting  $\Omega_R = 4.4\text{meV}$  determined experimentally, fixing the detuning to zero,  $\delta = \omega_C(0) - \omega_X(0) = 0$ . In the regime considered by the experiments, we can neglect the saturation of the dipole coupling [17]. We pump at  $\sim 12^\circ$  (corresponding to  $|\mathbf{k}_p| = 1.6\mu\text{m}^{-1}$  for a LPB energy at normal incidence of  $\omega_{LP}(0) = 1.524\text{eV}$ ). The energy of the pump  $\omega_p$  is tuned around 0.5meV above the bare LPB, in order to take into account the energy renormalisation due to interaction [18]. We have chosen a pump profile with full width at half maximum (FWHM) of  $35\mu\text{m}$ .

The pump strength  $f_p$  can be chosen to be below or above threshold for OPO. In particular, we consider two different situations in our numerical simulations. In one case we fix the pump strength  $f_p$  very close to the threshold for OPO,  $f_p = 0.999 f_p^{(\text{th})}$ . We switch on for 2ps only a probe with a  $m = 1, 2$  vortex with  $\sigma_{pb} = 4.5\mu\text{m}$ , momentum  $\mathbf{k}_{pb} = 0$  and energy  $\omega_{pb}$  around 0.5meV above the bare LPB dispersion. The probe triggers a signal, which intensity first quickly grows and then slowly decays in time—after 60ps the signal intensity is reduced by 2 orders of magnitude—. The vortex excited by the probe starts very slowly drifting inside the signal after 6ps and is visible for around 80ps.

In the second class of numerical simulations, we drive the system into the OPO regime at  $f_p = 1.12 f_p^{(\text{th})}$ , which generates a signal narrower than the pump with FWHM=12 $\mu\text{m}$  at slightly negative angles ( $\sim -2^\circ$ ). The signal is shifted parallel to the direction of the incident pumping laser of about  $5\mu\text{m}$  [15]. Once the steady state is reached for the pump only OPO configuration, we turn on the probe (Equation (2)) for 2ps only. The momentum  $\mathbf{k}_{pb}$  of the probe is tuned to the one of the OPO signal and its energy set around 0.5meV above the bare dispersion. We choose a probe with a vortex of  $m = 1$ . We have considered different sizes of the probe vortex, from  $2\sigma_{pb} = 9\mu\text{m}$  down to  $1\mu\text{m}$ . In addition, we shift the vortex core center to  $\mathbf{r}_{pb} = (4, 0)\mu\text{m}$ , in order to overlap the core with the maximum signal intensity. For the probe intensity we have considered different values in the range  $[1/200, 1]$  times the intensity of the pump, corresponding to a range of  $[1/20, 10]$  times the intensity of the signal. We have checked that neither the intensity nor the size of the probe changes qualitatively the outcome of the simulations. The existence of a stable vortex solution is independent on both the probe intensity and the probe size. Remarkably the signal rearranges itself

during the transient period and generate a stable vortex configuration with a vortex core size independent on the one of the probe. The transient period can last between  $[50, 300]$ ps, depending on the probe intensity and size. Our conclusion is that the probe can only change the quantitative behaviour and length of the transient period.

The calculated images of the signal in Figs. 3(a),(b), 4(g),(h) and 5(a),(b) are obtained by filtering in momentum space around the signal momentum,  $\mathbf{k}_s \simeq 0$ . We set to zero all the emission in momentum space aside the one coming from the signal and fast Fourier transform back to real space. In this way the strong emission coming at the pump angles is masked out. Interference fringes instead are obtained by taking the full emission without filtering out the pump (and the idler). In numerical simulations we consider a single shot measurement at a given time, therefore pump, signal and idler give rise to interference fringes, even if they oscillate at different energies. Such interferences are clearly washed out in experiments, where single shot measurements are hindered by the low signal to noise ratio. For this reason, in experiments we need to use a Michelson interferometer.

We are grateful to D. Whittaker, J.J. García-Ripoll, P. B. Littlewood and J. Keeling for stimulating discussions. This work was partially supported by the Spanish MEC (MAT2008-01555 and QOIT-CSD2006-00019), the CAM (S-0505/ESP-0200), and the IMDEA-Nanociencia. DS and FMM acknowledge financial support from the Ramón y Cajal programme. We would like to thank TCM group (Cavendish Laboratory, Cambridge, UK) for the use of computer resources.

## SUPPLEMENTARY MATERIAL

In Fig. 6 we show the intensity of the interference fringes of the vortex with  $m = 1$  (Fig. 2 of the main text) obtained with the Michelson interferometer but at different time delays between the two arms. Immediately after the probe has arrived, and at zero delay, the fringes exhibits a visibility close to 100%, while it reduces to 30% after a delay of 55ps. However the interferences of the vortex core of Fig. 2—taken always at zero delay time—do not show any degradation of the visibility even 80ps after the probe has arrived, demonstrating the persistence of the polariton vorticity.

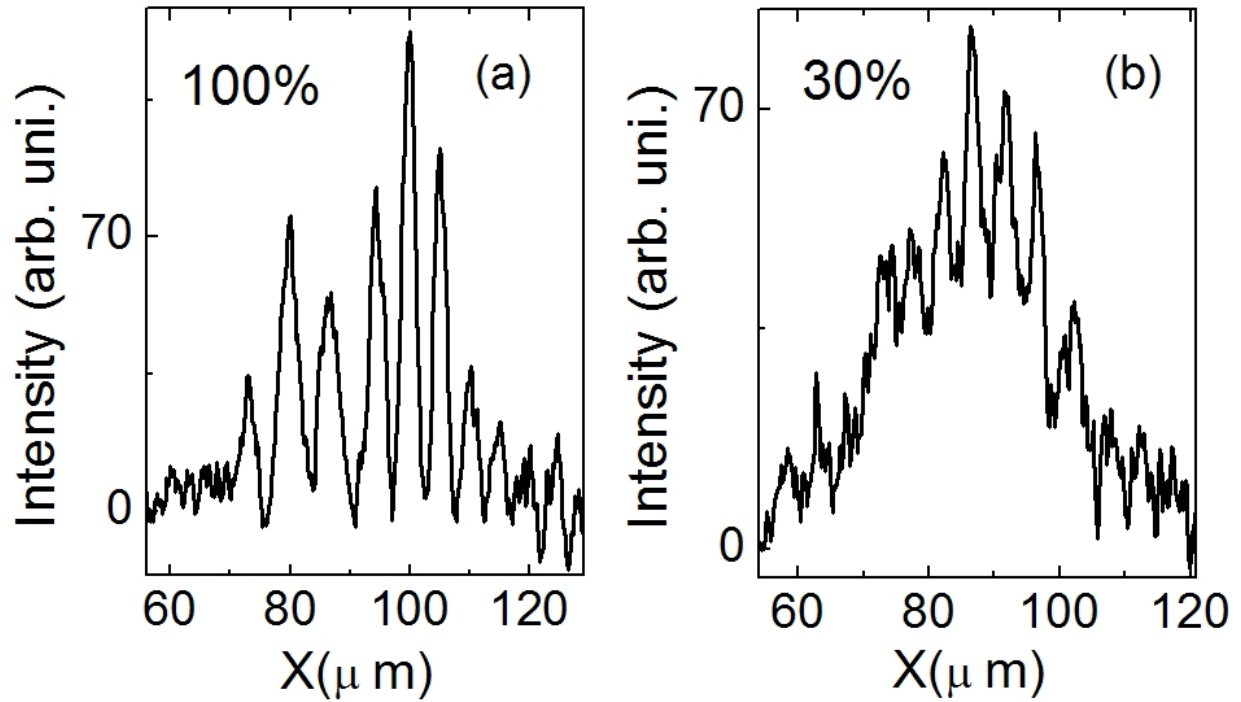


FIG. 6: Intensity of interference fringes (arbitrary units) of the polariton emission after arrival of the probe pulse. The two images are taken at different delay times between the polariton signal and its mirrored counterpart: (a) 0ps and (b) 55ps time delay.

---

\* Electronic address: daniele.sanvitto@uam.es

† Electronic address: francesca.marchetti@uam.es

‡ Electronic address: M.H.Szymanska@warwick.ac.uk

- [1] J. Kasprzak, et al., *Nature* **443** (2006).
- [2] C. Weisbuch, M. Nishioka, A. Ishikawa, and Y. Arakawa, *Phys. Rev. Lett.* **69**, 3314 (1992).
- [3] J. Keeling, F. M. Marchetti, M. H. Szymańska, and P. B. Littlewood, *Semicond. Sci. Technol.* **22**, R1 (2006).
- [4] J. Keeling and N. G. Berloff, *Nature* **457**, 273 (2009).
- [5] R. Balili, et al., *Science* **316**, 1007 (2007).
- [6] K. G. Lagoudakis, et al., *Nature Physics* **4**, 706 (2008).
- [7] M. H. Szymańska, J. Keeling, and P. B. Littlewood, *Phys. Rev. Lett.* **96**, 230602 (2006).
- [8] M. Wouters and I. Carusotto, *Phys. Rev. Lett.* **99**, 140402 (2007).
- [9] A. Amo, et al., *Nature* **457**, 291 (2009).
- [10] A. Amo, et al., *Nature physics*, to be published (2009).
- [11] R. M. Stevenson, et al., *Phys. Rev. Lett.* **85**, 3680 (2000).
- [12] Y. Shin, et al., *Phys. Rev. Lett.* **93**, 160406 (2004).
- [13] M. Baert, et al., *Phys. Rev. Lett.* **74**, 3269 (1995).
- [14] R. Blaauwgeers, et al., *Nature* **404**, 471 (2000).
- [15] D. Sanvitto, et al., *Phys. Rev. B* **73**, 241308 (2006).
- [16] D. Whittaker, *Superlatt. and Microstruct.* **41**, 297 (2007).
- [17] C. Ciuti, P. Schwendimann, and A. Quattropani, *Semicond. Sci. Technol.* **18**, S279 (2003).
- [18] D. M. Whittaker, *Phys. Rev. B* **71**, 115301 (2005).